双惯性伺服传动系统的抗扰动复合非线性控制

程国扬†, 黄宴委

(福州大学 电气工程与自动化学院, 福建 福州 350116)

摘要: 本文把复合非线性反馈(composite nonlinear feedback, CNF)控制技术推广到带有非定常扰动的输入饱和限幅的线性系统. 其中, 未知扰动被作为一个扩张状态量增广到被控对象的模型中, 然后设计一个扩展状态观测器来对系统的状态量和扰动同时进行估计, 通过在CNF控制的框架中引入一个扰动补偿机制, 在降低由扰动引起的稳态误差的同时, 保留了CNF原有的快速的瞬态性能. 这种控制方案对定常或时变扰动、匹配或非匹配的扰动, 都能统一处理. 论文对该控制方案的闭环稳定性和定点跟踪性能进行了理论分析, 并把它应用到一个双惯性伺服传动系统. 数值仿真结果验证了该方案在定点跟踪控制中具有优越的瞬态性能和稳态精度, 且对扰动/给定目标的幅值变化也有一定的性能鲁棒性.

关键词: 运动控制; 非线性反馈; 抗扰动; 观测器; 瞬态性能

中图分类号: TP273 **文献标识码:** A

Disturbance-rejection composite nonlinear control applied to two-inertia servo drive system

CHENG Guo-yang†, HUANG Yan-wei

(College of Electrical Engineering and Automation, Fuzhou University, Fuzhou Fujian 350116, China)

Abstract: This paper extends the composite nonlinear feedback (CNF) control method to linear systems subject to input saturation and non-constant disturbance. The unknown disturbance is treated as an extended state variable to be augmented with the plant model, and then an extended state observer is designed to estimate both the states and the disturbance, and a disturbance compensation mechanism is incorporated into the CNF framework, so as to alleviate the steady-state bias due to disturbances, while retaining the fast transient performance of the original CNF control. Both constant and varying disturbances, either matched or unmatched, can be handled within this control scheme. Closed-loop stability and set-point tracking performance are analyzed theoretically. The proposed control scheme is then applied to a two-inertia servo drive system. Simulation studies are conducted to verify its superior transient performance and steady-state accuracy in set-point tracking, as well as the robustness against the amplitude variations of disturbance/set-point.

Key words: motion control; nonlinear feedback; disturbance-rejection; observer; transient performance

1 Introduction

Rapid motion control is required in many industrial applications, for which myriad advanced control techniques have been developed to achieve faster and more precise position or velocity regulation (see e.g., [1–5]). So far, linear control techniques have gained popularity in most applications. However, it is well know that a linear control system with a given bandwidth cannot achieve fast response while maintaining a low overshoot, and a tradeoff always needs to be made. In the seminal paper [6], Lin et al. proposed an add-in nonlinear feedback term to supplement the linear state feedback control law so as to speed up the settling process of set-point tracking tasks for second order linear systems with input amplitude constraint. Chen et al.[7] extended this idea and developed the so-called compos-

ite nonlinear feedback (CNF) control technique, for more general linear systems with measurement feedback and input saturation but without external disturbances. The CNF control consists of a linear control part and a nonlinear feedback part. The linear control part is designed such that the closed-loop system yields a fast response. Generally, a pair of dominant poles is designed to have a small damping ratio. The nonlinear feedback portion is then designed to tune the damping ratio of the closed-loop system when the system controlled output approaches the target reference to gradually reduce the overshoot resulted from the linear control law. Thus, the CNF implements a closed-loop dynamics from lightly damped to heavily damped, leading to fast and smooth transient response in set-point tracking tasks. So far, successful implementations of CNF have

been reported on disk drive servo test-beds (see e.g., [7–9]) and unmanned helicopters (see e.g., [10–12]).

In the earlier development of CNF, it was assumed that no disturbances exist in the plant. When the given plant does have disturbances, the resulting system output with CNF control generally cannot asymptotically match the target reference. In typical servo applications, there are always some disturbances, e.g., friction and load torques. Under such circumstance, the original CNF technique alone cannot achieve accurate servo tracking. To remove the steady-state bias caused by unknown constant disturbances, Peng et al.[8] enhanced the CNF technique with an additional integration action. The headache with integral control is that it can easily lead to the so-called integral-windup phenomenon. Moreover, it is found that integral control is not robust to the amplitude of disturbance and/or target reference, e.g., a minor change in the amplitude of disturbance or target may call for a re-tuning of controller parameters in order to maintain a satisfactory performance. This is undesirable for practical applications. To gain a better robustness against the amplitudes of reference and disturbance, Cheng et al.[13] incorporated an extended state observer (ESO) into the CNF control framework, where the unknown constant disturbance is estimated together with the unmeasurable state variables. Because of the disturbance compensation, the expected value of system state is no longer constant compared to that in the original CNF control. Such a flexibility helps to improve the robustness against disturbances. However, [8, 13] assume a constant disturbance, which may be an over-simplification for some practical systems, e.g., the frictional disturbance usually exhibits some dynamic behaviors, such as hysteresis. This motivated us to extend the result in [13] to cover more general systems subject to input saturation and a time-varying unknown disturbance. Theoretical analysis will show that the ultimate bounded-ness of tracking error can be guaranteed for a rate-bounded disturbance, and moreover, a zero steady-state error will be achieved in the case of constant disturbance.

The rest of the paper is organized as follows. The design of disturbance-rejection CNF control is presented in Section 2. Section 3 is devoted to the theoretical analysis of closed-loop system. In Section 4, the effectiveness of the proposed control scheme is demonstrated on a two-inertial servo drive system. Some concluding remarks are provided in Section 5.

2 Disturbance-rejection CNF control

In this section we present a robust version of the CNF control design, which incorporates an extended state observer to estimate the unknown disturbances together with unmeasurable state variables, and a disturbance compensation mechanism is subsequently designed to improve the tracking accuracy in servo systems. The new approach will retain the quick response property of the original CNF control and at the same time have an additional capacity of reducing steady-state bias caused by disturbances yet without resorting to explicit integration control. It should be noted that this design is an extension to the work reported

in [13], where the disturbance was limited to a constant one. Here, we consider a linear system subject to an amplitude constrained actuator and an unknown bounded disturbance with a limited rate of change, characterized by

$$
\begin{cases}
\dot{x} = Ax + B\text{sat}\,u + Ew,\ x(0) = x_0, \\
y = C_1 x, \\
h = C_2 x,
\end{cases}
\tag{1}
$$

where $x \in \mathbb{R}^n$, $u \in \mathbb{R}$, $y \in \mathbb{R}^p$, $h \in \mathbb{R}$ and $w \in \mathbb{R}$ are respectively the state, control input, measurement output, controlled output and disturbance input of the system. A, B, C_1, C_2 and E are constant matrices of appropriate dimensions. The function, sat: $\mathbb{R} \to \mathbb{R}$, represents the actuator saturation defined as

$$
\text{sat}\,u = \text{sgn}\,u \cdot \min\{u_{\max}, |u|\}
\tag{2}
$$

with $u_{\max}$ being the saturation level of the input. The following assumptions on the given system are made:

    1) (A, B) is stabilizable.

    2) (A, C_1) is detectable.

    3) (A, B, C_2) and (A, E, C_1) have no zeros at $s = 0$.

    4) w is an unknown bounded disturbance with a limited variation rate.

    5) h is a subset of y, i.e., h is also measurable.

Note the above assumptions are fairly standard for tracking control. We aim to design a robust control law without explicit integration action for the given system such that the resulting controlled output would track a set-point target reference, say r, fast, smoothly, and accurately as possible.

In the following, we outline the design procedure of the proposed control scheme, which involves 4 major steps.

Step 1   Design a linear disturbance-rejection control law for the system (10) as follows:

$$
u_{\text{L}} = Fx + F_{\text{w}}w + Gr,
\tag{3}
$$

where F is chosen such that 1) $A + BF$ is Hurwitz, and 2) the transfer function $C_2(sI - A - BF)^{-1}B$ has a dominant pair of conjugate poles with a small damping ratio, which would lead to a fast closed-loop output response. Next, the feed-forward gain G is chosen as

$$
G = -[C_2(A + BF)^{-1}B]^{-1},
\tag{4}
$$

and F_{w} is then determined as

$$
F_{\text{w}} = G[C_2(A + BF)^{-1}E],
\tag{5}
$$

which are well defined as $C_2(sI - A - BF)^{-1}B$ has no zeros at $s = 0$. Note that the state variables and the disturbance term in the control law will eventually be replaced with their respective estimated ones.

Step 2   Given a positive definite symmetric matrix $W \in \mathbb{R}^{n \times n}$, we solve the following Lyapunov equation:

$$
(A + BF)'P + P(A + BF) = -W,
\tag{6}
$$

for $P > 0$. Such a solution is always existent as $(A + BF)$ is asymptotically stable. Next, we define

$$
\begin{cases}
G_{\text{e}} := -(A + BF)^{-1}BG, \\
G_{\text{w}} := -(A + BF)^{-1}(BF_{\text{w}} + E),
\end{cases}
\tag{7}
$$

and the expected value of system state

$$x_{\mathrm{e}} := G_{\mathrm{e}} r + G_{\mathrm{w}} w. \tag{8}$$

It is then trivial to verify that $C_2 x_{\mathrm{e}} = r$. The nonlinear feedback control law, u_{N}, can now be given by

$$u_{\mathrm{N}} = \rho(e) F_{\mathrm{n}}(x - x_{\mathrm{e}}), \tag{9}$$

where $F_{\mathrm{n}} = B'P$, and $\rho(e)$ is a smooth, non-positive function of $|e|$ with $e = h - r$, to be used to gradually change the system closed-loop damping ratio to yield a better tracking performance. The choices of the design parameters, $\rho(e)$ and W, will be discussed later.

Step 3 An observer will be designed to estimate the state variables and unknown disturbance. Here we assume that the measurement output matrix $C_1 \in \mathbb{R}^{p \times n}$ is of full row rank, i.e., there is no redundancy in the measurements. Choose a matrix $C_0 \in \mathbb{R}^{(n-p) \times n}$, such that the matrix $T = \begin{bmatrix} C_1 \\ C_0 \end{bmatrix}$ is invertible. Define the extended state vector $\bar{x} = \begin{pmatrix} Tx \\ w \end{pmatrix}$ and obtain an augmented model as follows:

$$\begin{cases} \dot{\bar{x}} = \bar{A} \cdot \bar{x} + \bar{B} \cdot \mathrm{sat}\, u + N \cdot \dot{w}, \\ y = \bar{C}\, \bar{x}, \end{cases} \tag{10}$$

where

$$\bar{A} = \begin{bmatrix} TAT^{-1} & TE \\ 0 & 0 \end{bmatrix}, \quad \bar{B} = \begin{bmatrix} TB \\ 0 \end{bmatrix},$$

$$N = \begin{bmatrix} 0 \\ 1 \end{bmatrix}, \quad \bar{C} = \begin{bmatrix} I_p & 0 \end{bmatrix}.$$

Based on the assumptions about the plant model, it is easy to check $(\bar{C}, \bar{A})$ is detectable. Thus, an observer, of either full order or reduced order, can be designed to estimate the extended state variables. In real-time control, it is more feasible to implement controllers with smaller dynamical order. Clearly, the first p elements of extended state vector, denoted by $\bar{x}_1$, is readily available from the measurement output y. We only need to estimate the remaining $n - p + 1$ elements of state vector, denoted by $\bar{x}_2$, and the matrices in the augmented model (10) can then be partitioned in accordance with the dimensions of $\bar{x}_1$ and $\bar{x}_2$, as follows:

$$\bar{A} = \begin{bmatrix} A_{11} & A_{12} \\ A_{21} & A_{22} \end{bmatrix}, \quad \bar{B} = \begin{bmatrix} B_1 \\ B_2 \end{bmatrix}, \quad N = \begin{bmatrix} 0 \\ N_1 \end{bmatrix}.$$

Following the design procedure of reduced-order observer in [8], we choose an observer gain matrix $K \in \mathbb{R}^{(n-p+1) \times p}$ such that the poles of $A_{22} + KA_{12}$ are placed in appropriate locations in the open-left half plane. Then the reduced-order observer is derived as

$$\begin{cases} \dot{x}_{\mathrm{v}} = A_{\mathrm{v}} \cdot x_{\mathrm{v}} + B_{\mathrm{u}} \cdot \mathrm{sat}\, u + B_{\mathrm{y}} \cdot y, \\ \hat{\bar{x}}_2 = x_{\mathrm{v}} - Ky, \end{cases} \tag{11}$$

where x_{v} is the internal state vector of the observer, and $\hat{\bar{x}}_2$ is the estimation of $\bar{x}_2$. Further

$$\begin{cases} A_{\mathrm{v}} = A_{22} + KA_{12}, \\ B_{\mathrm{u}} = B_2 + KB_1, \\ B_{\mathrm{y}} = A_{21} + KA_{11} - (A_{22} + KA_{12})K. \end{cases}$$

The estimation of extended state vector $\bar{x}$ is given by

$$\hat{\bar{x}} = \begin{pmatrix} y \\ x_{\mathrm{v}} - Ky \end{pmatrix}.$$

The estimations of the original state vector x and unknown disturbance w can be obtained as

$$\begin{cases} \hat{x} = T^{-1} \begin{bmatrix} I_n & 0 \end{bmatrix} \hat{\bar{x}}, \\ \hat{w} = \begin{bmatrix} 0 & \cdots & 0 & 1 \end{bmatrix} \hat{\bar{x}}. \end{cases} \tag{12}$$

Step 4 In this step, the linear control law, the nonlinear feedback portion, and the extended state observer derived in the previous steps are combined to form the final controller

$$u = \begin{bmatrix} F & F_{\mathrm{w}} \end{bmatrix} \begin{pmatrix} \hat{x} \\ \hat{w} \end{pmatrix} + Gr + \rho(e) F_{\mathrm{n}} \left(\hat{x} - G_{\mathrm{e}} r - G_{\mathrm{w}} \hat{w} \right), \tag{13}$$

where the estimated values $\hat{x}$ and $\hat{w}$ are given in (12).

Remark 1 Figure 1 is a schematic of the control system, where the linear control law is a fundamental part, comprising the state feedback and feed-forward compensation of reference and disturbance, while the nonlinear feedback part serves to tune up the dominant closed-loop damping ratio for suppressing overshoot. The extended state observer (ESO) provides a unified mechanism for state and disturbance estimation. Both matched and unmatched disturbances can be handled within this framework. The idea of using observer to estimate both state and disturbance has been available for quite some time and is still attracting the attention from the control community (see e.g., [14–18]). The conventional ESO design assumes a constant or slowly varying disturbance, i.e., its variation rate is reasonably small. If the variation rate is not negligible but is bounded anyway, then the observer error will remain bounded with an upper bound monotonously decreasing with the increase in the observer bandwidth [19]. For time-varying disturbances, an improved estimation is possible by resorting to the generalized ESO, or higher order ESO (see e.g., [20–21]).

Remark 2 The procedures for selecting the design parameter W and the nonlinear gain $\rho(e)$ for the control scheme here are basically the same as those given in [7–8]. By the theory of root locus, the closed-loop poles of CNF control system approach the locations of the invariant zeros of $G_{\mathrm{aux}}(s)$:

$$G_{\mathrm{aux}}(s) := F_{\mathrm{n}}(sI - A - BF)^{-1}B, \tag{14}$$

as $|\rho|$ gets larger. Note that the locations of these invariant zeros are highly dependent on the choice of matrix W. In general, an appropriate $W > 0$ should be chosen such that the invariant zeros of $G_{\mathrm{aux}}(s)$, have a dominant pair with a large damping ratio, which in turn will yield a smaller overshoot. A software toolkit for CNF control design has been reported in [22].

Remark 3 The general guideline for selecting the nonlinear function $\rho(e)$ is that it should be a smooth, non-positive and non-decreasing function of $|e|$. Several forms of nonlinear function $\rho(e)$ have been suggested in [6–9]. Especially, the one proposed in [9] is a scaled nonlinear function with a better performance robustness to variation of tracking targets:

$$\rho(e) = -\beta \mathrm{e}^{-\alpha \alpha_0 |e|}, \tag{15}$$

with

$$\alpha_0 = \begin{cases} \dfrac{1}{|e(0)|}, & \text{if } e(0) \neq 0, \\ 1, & \text{if } e(0) = 0, \end{cases}$$

in which α and β are positive scalars that can be tuned to improve tracking performances. An auto-tuning procedure for parameter α and β using the Hooke-Jeeves method is proposed in [9]. It should be noted that the choice of $\rho(e)$ is non-unique.
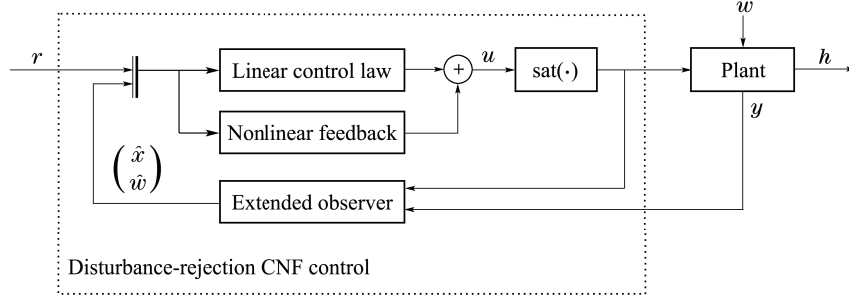
Fig. 1 Schematic diagram of the proposed control scheme

3 Stability analysis

To analyze the closed-loop stability, let us first partition the matrix $T^{-1} = \begin{bmatrix} T_1 & T_2 \end{bmatrix}$ such that T_1 has p columns. Define

$$H = G + FG_e, \ H_w = F_w + FG_w,$$

$$F_v = \begin{bmatrix} FT_2 & F_w \end{bmatrix}, \ F_{nv} = \begin{bmatrix} F_nT_2 & -F_nG_w \end{bmatrix},$$

and

$$\tilde{x} = x - x_e, \ z = \hat{\bar{x}}_2 - \bar{x}_2.$$

It is easy to verify that

$$\begin{pmatrix} \hat{x} - x \\ \hat{w} - w \end{pmatrix} = \begin{bmatrix} T_2 & 0 \\ 0 & 1 \end{bmatrix} z. \tag{16}$$

Then the control law in (13) can be rewritten as

$$u = \begin{bmatrix} F & F_v \end{bmatrix} \begin{pmatrix} \tilde{x} \\ z \end{pmatrix} + \begin{bmatrix} H & H_w \end{bmatrix} \begin{pmatrix} r \\ w \end{pmatrix} + \rho(e) \begin{bmatrix} F_n & F_{nv} \end{bmatrix} \begin{pmatrix} \tilde{x} \\ z \end{pmatrix}. \tag{17}$$

Next, we choose a positive definite matrix $M \in \mathbb{R}^{(n-p+1)\times(n-p+1)}$ such that

$$M > F_v'B'PW^{-1}PBF_v, \tag{18}$$

and solve the following Lyapunov equation

$$A_v'Q + QA_v = -M \tag{19}$$

for a positive definite matrix Q. Note that such a Q exists as $A_v = A_{22} + KA_{12}$ is asymptotically stable. We have the following result.

Theorem 1 For the given system (1) with the unknown disturbance w, there exists a scalar $\rho^* > 0$ such that for any $\rho(e)$, which is a smooth, non-positive function of $|e|$ with $|\rho(e)| \leqslant \rho^*$, the observer-based disturbance-rejection CNF control law of (13) will ensure the stability of the closed-loop system and that the system controlled output h will approach the step reference r without steady-state error if the disturbance w is constant, or with a bounded tracking error if the variation rate of w is bounded by a non-negative scalar τ_w (i.e., $|\dot{w}| \leqslant \tau_w$), provided that the following conditions are satisfied:

1) There exist two positive scalars $\delta \in (0, 1)$ and $c_\delta > 0$ such that

$$\forall \xi \in \Omega(\delta, c_\delta) := \{\xi \in \mathbb{R}^{2n-p+1} : \xi' \begin{bmatrix} P & 0 \\ 0 & Q \end{bmatrix} \xi \leqslant c_\delta\} \Rightarrow$$

$$\left| \begin{bmatrix} F & F_v \end{bmatrix} \xi \right| \leqslant (1 - \delta)u_{max}. \tag{20}$$

2) The initial conditions, $x_0 = x(0)$, $w(0)$, and $x_v(0)$, satisfy

$$\begin{pmatrix} \tilde{x}(0) \\ z(0) \end{pmatrix} \in \Omega(\delta, c_\delta). \tag{21}$$

3) The target reference r, and the disturbance w, satisfy

$$|Hr + H_w w| \leqslant \delta \cdot u_{max}. \tag{22}$$

Proof First, it is easy to derive the observer error dynamics as follows:

$$\dot{z} = A_v \cdot z - N_1\dot{w}. \tag{23}$$

Next, we note that

$$(A + BF)x_e + BGr + (BF_w + E)w = 0. \tag{24}$$

By applying (24) and the definitions of error variables, the error dynamics of plant (1) can be expressed as follows:

$$\dot{\tilde{x}} = Ax + B\text{sat } u + Ew - G_w\dot{w} = (A + BF)\tilde{x} + BF_vz + Bv - G_w\dot{w}, \tag{25}$$

where

$$v := \text{sat } u - \begin{bmatrix} F & F_v \end{bmatrix} \begin{pmatrix} \tilde{x} \\ z \end{pmatrix} - \begin{bmatrix} H & H_w \end{bmatrix} \begin{pmatrix} r \\ w \end{pmatrix}. \tag{26}$$

To simplify the presentation, we will drop the variable e of function $\rho(e)$ throughout this proof. It is noted that, for $\begin{pmatrix} \tilde{x} \\ z \end{pmatrix} \in \Omega(\delta, c_\delta)$ and $|Hr + H_w w| \leqslant \delta u_{max}$, we have

$$\left| \begin{bmatrix} F & F_v \end{bmatrix} \begin{pmatrix} \tilde{x} \\ z \end{pmatrix} + \begin{bmatrix} H & H_w \end{bmatrix} \begin{pmatrix} r \\ w \end{pmatrix} \right| \leqslant$$

$$\left| \begin{bmatrix} F & F_v \end{bmatrix} \begin{pmatrix} \tilde{x} \\ z \end{pmatrix} \right| + |Hr + H_w w| \leqslant u_{max}. \tag{27}$$

Following the similar reasoning in [7], we can show for the three possible situations of $u < -u_{max}$, $|u| \leqslant u_{max}$ and $u > u_{max}$, the variable v can always be rewritten as

$$v = q\rho \begin{bmatrix} F_n & F_{nv} \end{bmatrix} \begin{pmatrix} \tilde{x} \\ z \end{pmatrix}, \tag{28}$$

for some non-negative variable $q \in [0, 1]$. Thus, for the case when $\begin{pmatrix} \tilde{x} \\ z \end{pmatrix} \in \Omega(\delta, c_\delta)$ and $|Hr + H_w w| \leqslant \delta u_{max}$, the closed-loop system comprising the given plant (1) and the observer-based control law (13) can be expressed as follows:

$$\begin{pmatrix} \dot{\tilde{x}} \\ \dot{z} \end{pmatrix} = \begin{bmatrix} A+BF+q\rho BF_n & B(F_v+q\rho F_{nv}) \\ 0 & A_v \end{bmatrix} \begin{pmatrix} \tilde{x} \\ z \end{pmatrix} - \begin{bmatrix} G_w \\ N_1 \end{bmatrix} \dot{w}. \tag{29}$$

In what follows, we will show that closed-loop system (29) is stable provided that the initial condition, $x(0)$ and

$x_{\mathrm{v}}(0)$, the target reference, r, and the disturbance, w, satisfy those conditions listed in Theorem 1. Let us define a Lyapunov function

$$V = \begin{pmatrix} \tilde{x} \\ z \end{pmatrix}' \begin{bmatrix} P & 0 \\ 0 & Q \end{bmatrix} \begin{pmatrix} \tilde{x} \\ z \end{pmatrix}. \tag{30}$$

The derivative of V is then calculated along the trajectory of the system (29):

$$\begin{aligned}
\dot{V} = {} & \tilde{x}'[(A+BF)'P+P(A+BF)]\tilde{x}+2q\rho\tilde{x}'PBF_{\mathrm{n}}\tilde{x}+ \\
& 2\tilde{x}'PB(F_{\mathrm{v}}+q\rho F_{\mathrm{nv}})z - 2\tilde{x}'PG_{\mathrm{w}}\dot{w} - \\
& z'(A_{\mathrm{v}}'Q+QA_{\mathrm{v}})z - 2z'QN_1\dot{w} \leqslant \\
& -\tilde{x}'W\tilde{x}+2\tilde{x}'PB(F_{\mathrm{v}}+q\rho F_{\mathrm{nv}})z - z'Mz - \\
& 2\tilde{x}'PG_{\mathrm{w}}\dot{w} - 2z'QN_1\dot{w} = \\
& -\begin{pmatrix} \tilde{x} \\ z \end{pmatrix}' W_\rho \begin{pmatrix} \tilde{x} \\ z \end{pmatrix} - 2\begin{pmatrix} \tilde{x} \\ z \end{pmatrix}' \begin{bmatrix} P & 0 \\ 0 & Q \end{bmatrix} \begin{bmatrix} G_{\mathrm{w}} \\ N_1 \end{bmatrix} \dot{w}, \tag{31}
\end{aligned}$$

where

$$W_\rho = \begin{bmatrix} W & -PB(F_{\mathrm{v}}+q\rho F_{\mathrm{nv}}) \\ -(F_{\mathrm{v}}+q\rho F_{\mathrm{nv}})'B'P & M \end{bmatrix}. \tag{32}$$

According to the definition of M in (18), there exists a scalar $\rho^* > 0$ such that for any $\rho(e)$, which is a smooth, non-positive function of $|e|$ with $|\rho(e)| \leqslant \rho^*$, we have $W_\rho > 0$.

For easy derivation, we define

$$x_{\mathrm{z}} := \begin{pmatrix} \tilde{x} \\ z \end{pmatrix}, \ P_{\mathrm{Q}} := \begin{bmatrix} P & 0 \\ 0 & Q \end{bmatrix}, \ N_{\mathrm{w}} := \begin{bmatrix} G_{\mathrm{w}} \\ N_1 \end{bmatrix},$$

$$\lambda_{\mathrm{m}} := \max\{\lambda_{\max}(P_{\mathrm{Q}}W_\rho^{-1}) : 0 \leqslant \rho \leqslant \rho^*\},$$

$$\gamma := 2\tau_{\mathrm{w}}\lambda_{\mathrm{m}}(G_{\mathrm{w}}'PG_{\mathrm{w}} + N_1'QN_1)^{1/2}.$$

By introducing a square matrix S such that $P_{\mathrm{Q}} = S'S$, we will have the following:

$$\begin{aligned}
\dot{V} \leqslant {} & -x_{\mathrm{z}}'S'SP_{\mathrm{Q}}^{-1}W_\rho P_{\mathrm{Q}}^{-1}S'Sx_{\mathrm{z}} - 2x_{\mathrm{z}}'S'SN_{\mathrm{w}}\dot{w} \leqslant \\
& -\lambda_{\min}(SP_{\mathrm{Q}}^{-1}W_\rho P_{\mathrm{Q}}^{-1}S')x_{\mathrm{z}}'S'Sx_{\mathrm{z}} + \\
& 2\|Sx_{\mathrm{z}}\| \cdot \|SN_{\mathrm{w}}\|\tau_{\mathrm{w}} = -\lambda_{\min}(P_{\mathrm{Q}}^{-1}W_\rho)x_{\mathrm{z}}'P_{\mathrm{Q}}x_{\mathrm{z}} + \\
& 2\tau_w(x_{\mathrm{z}}'P_{\mathrm{Q}}x_{\mathrm{z}})^{1/2}(N_{\mathrm{w}}'P_{\mathrm{Q}}N_{\mathrm{w}})^{1/2} = \\
& -\lambda_{\min}(P_{\mathrm{Q}}^{-1}W_\rho)(x_{\mathrm{z}}'P_{\mathrm{Q}}x_{\mathrm{z}})^{1/2} \times \\
& \left[(x_{\mathrm{z}}'P_{\mathrm{Q}}x_{\mathrm{z}})^{1/2} - 2\tau_{\mathrm{w}}\lambda_{\max}(P_{\mathrm{Q}}W_\rho^{-1})(N_{\mathrm{w}}'P_{\mathrm{Q}}N_{\mathrm{w}})^{1/2}\right] \leqslant \\
& -\lambda_{\min}(P_{\mathrm{Q}}^{-1}W_\rho)(x_{\mathrm{z}}'P_{\mathrm{Q}}x_{\mathrm{z}})^{1/2} \times [(x_{\mathrm{z}}'P_{\mathrm{Q}}x_{\mathrm{z}})^{1/2} - \gamma].
\end{aligned}$$

Clearly, the closed-loop system with a constant disturbance, i.e., $\tau_{\mathrm{w}} = 0$, has $\dot{V} < 0$ and thus is asymptotically stable. As $\tilde{x} \to 0$, $h = C_2x \to C_2x_{\mathrm{e}} = r$, implying that the system output h approaches the set-point target r without steady-state error.

In the presence of a time-varying disturbance ($\tau_{\mathrm{w}} > 0$), and with $\begin{pmatrix} \tilde{x}(0) \\ z(0) \end{pmatrix} \in \Omega(\delta, c_\delta)$, where $c_\delta > \gamma^2$, the corresponding trajectory of (29) will remain in $\Omega(\delta, c_\delta)$ and eventually settle into a ball characterized by $\{ \begin{pmatrix} \tilde{x} \\ z \end{pmatrix} : \begin{pmatrix} \tilde{x} \\ z \end{pmatrix}' \begin{bmatrix} P & 0 \\ 0 & Q \end{bmatrix} \begin{pmatrix} \tilde{x} \\ z \end{pmatrix} \leqslant \tilde{\gamma}^2 \}$ with $\tilde{\gamma} \leqslant \gamma$. Thus

$$\tilde{\gamma}^2 \geqslant \tilde{x}'P\tilde{x} \geqslant \lambda_{\min}(P) \cdot \|\tilde{x}\|^2$$

or

$$\|\tilde{x}\| \leqslant \frac{\tilde{\gamma}}{\sqrt{\lambda_{\min}(P)}}.$$

Note that the tracking error $e = h - r = C_2\tilde{x}$, hence

$$|e| = |C_2\tilde{x}| \leqslant \|C_2\| \cdot \|\tilde{x}\| \leqslant \frac{\tilde{\gamma}\|C_2\|}{\sqrt{\lambda_{\min}(P)}}.$$

Obviously, the tracking error $e(t)$ is ultimately bounded. This completes the proof of Theorem 1.

Remark 4 Based on the Eq.(17), the control signal u can be decomposed into three components: the one dependent on state error, the one related to observer error, and finally, the one corresponding to exogenous signals r and w. The term $Hr + H_{\mathrm{w}}w$ in Eq.(22) actually represents the steady-state control signal when the state error and observer error converge to negligible values. Obviously, its amplitude should be smaller than $u_{\max}$, otherwise even the maximum control signal would be insufficient to counteract the disturbance and target reference, leaving no control energy for servo tracking tasks. Theorem 1 assumes that $Hr + H_{\mathrm{w}}w$ is bounded by $\delta \cdot u_{\max}$, thus in the worst case there is a remaining control energy of $(1 - \delta)u_{\max}$ to overcome the observer error and perform servo tracking.

4 Application to a two-inertia servo system

In this section, we apply the proposed control method to a two-inertia servo drive system with resilient coupling. Such kind of systems can be found in many industrial applications. So far, control design for two-inertia servo drive systems has attracted a lot of research efforts, mostly related to the PID–type techniques (see e.g., [23–25]). The difficulty in dealing with such systems is the unmatched load torque acting on the load machine. However, the disturbance-rejection CNF control will prove to be a good solution for such case.

Figure 2 shows a schematic of a two-inertia servo-drive system consisting of two lumped inertias J_{m} and J_{d}, representing the motor and load, respectively, coupled via a shaft of finite stiffness k_{c}. This shaft is subjected to a torsional torque τ_{s} and excited by a combination of electromagnetic torque τ_{e} and load-torque perturbations τ_{L}. The considered system could be described by the following dynamics equation:

$$\begin{cases} \dfrac{\mathrm{d}\omega_{\mathrm{m}}}{\mathrm{d}t} = \dfrac{1}{J_{\mathrm{m}}}(\tau_{\mathrm{e}} - \tau_{\mathrm{s}}), \\ \dfrac{\mathrm{d}\omega_{\mathrm{d}}}{\mathrm{d}t} = \dfrac{1}{J_{\mathrm{d}}}(\tau_{\mathrm{s}} - \tau_{\mathrm{L}}), \\ \dfrac{\mathrm{d}\tau_{\mathrm{s}}}{\mathrm{d}t} = k_{\mathrm{c}}(\omega_{\mathrm{m}} - \omega_{\mathrm{d}}), \end{cases} \tag{33}$$

where ω_{m} is the motor speed, ω_{d} is the load speed, τ_{e} is the electromagnetic torque of motor, τ_{s} is the shaft torque (torsional), τ_{L} is the disturbance torque, $J_{\mathrm{m}} = 0.0058 \ \mathrm{N \cdot m^2}$ and $J_{\mathrm{d}} = 0.00145 \ \mathrm{N \cdot m^2}$ are the lumped inertias of the motor and the load machine respectively, and $k_{\mathrm{c}} = 110 \ (\mathrm{N \cdot m})/\mathrm{rad}$ is the stiffness of the resilient coupling [23]. The electromagnetic torque τ_{e} is used as the control input of the system, and the angular speed ω_{d} of the load machine is taken as the system output to be controlled. ω_{m}

and ω_d are assumed to be measurable. The above model can be cast into the standard form of (1), with

$$x = \begin{pmatrix} \omega_m \\ \omega_d \\ \tau_s \end{pmatrix}, \ y = \begin{pmatrix} \omega_m \\ \omega_d \end{pmatrix}, \ h = \omega_d, \ u = \tau_e, \ w = \tau_L,$$

and

$$A = \begin{bmatrix} 0 & 0 & -\dfrac{1}{J_m} \\ 0 & 0 & \dfrac{1}{J_d} \\ k_c & -k_c & 0 \end{bmatrix}, \ B = \begin{bmatrix} \dfrac{1}{J_m} \\ 0 \\ 0 \end{bmatrix}, \ E = \begin{bmatrix} 0 \\ -\dfrac{1}{J_d} \\ 0 \end{bmatrix},$$

$$C_1 = \begin{bmatrix} 1 & 0 & 0 \\ 0 & 1 & 0 \end{bmatrix}, C_2 = [0 \ 1 \ 0].$$
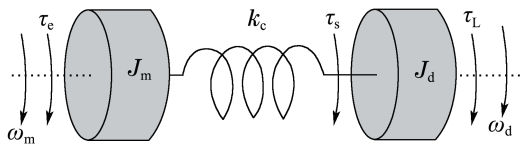
Fig. 2 Mechanical schematic of a two-inertia system

The saturation level of τ_e is assumed to be $u_{max} = 20$ N·m. The objective in control design is for the angular speed ω_d of the load machine to track a given set-point target speed r fast, smoothly and accurately.

Following the design procedure outlined previously, we first design a linear control law

$$u_L = [F \ F_w] \begin{pmatrix} x \\ w \end{pmatrix} + Gr =$$
$$[-5.336 \ 3.501 \ -7.233 \ 8.233] \begin{pmatrix} x \\ w \end{pmatrix} + 1.835r, \tag{34}$$

which places the closed-loop poles at $-\zeta\omega_n \pm j\omega_n\sqrt{1-\zeta^2}$ and $-3\omega_n$ with $\zeta = 0.3$ and $\omega_n = 200$ rad/s. Next, we choose the matrix W to be the third-order identity matrix and solve the Lyapunov equation in (6) for matrix P:

$$P = \begin{bmatrix} 1.408 & 1.753 & 7.234 \\ 1.753 & 8.071 & 14.16 \\ 7.234 & 14.16 & 67.68 \end{bmatrix} \times 10^{-3}, \tag{35}$$

we then obtain the nonlinear feedback part of CNF as follows:

$$u_N = \rho(e)F_n(x - G_e r - G_w w) \tag{36}$$

with

$$F_n = B'P = [0.2428 \ 0.3022 \ 1.247],$$
$$G_e = \begin{bmatrix} 1 \\ 1 \\ 0 \end{bmatrix}, \ G_w = \begin{bmatrix} 0 \\ 0 \\ 1 \end{bmatrix},$$

and $\rho(e)$ is as given in (15) with $e = \omega_d - r$ and $\alpha = 1$, $\beta = 25$.

Next, to estimate the unmeasured shaft torque τ_s and the unknown disturbance w (i.e., the load τ_L), we design a reduced-order extended state observer with its two poles organized in Butterworth pattern and with a bandwidth of $\omega_v = 800$ rad/s. Combining all the above results, we arrive at the following disturbance-rejection CNF controller

(referred to as RCNF later) for the servo system:

$$\begin{cases} \dot{x}_v = \begin{bmatrix} -565.7 & 565.7 \\ -565.7 & -565.7 \end{bmatrix} x_v + \begin{bmatrix} 0 \\ 1131.4 \end{bmatrix} \text{sat } u + \\ \qquad \begin{bmatrix} -3602 & -1038 \\ 3712 & 0 \end{bmatrix} \begin{pmatrix} \omega_m \\ \omega_d \end{pmatrix}, \\ \begin{pmatrix} \hat{\tau}_s \\ \hat{w} \end{pmatrix} = x_v + \begin{bmatrix} 0 & -0.8202 \\ 6.562 & 0.8202 \end{bmatrix} \begin{pmatrix} \omega_m \\ \omega_d \end{pmatrix}, \end{cases} \tag{37}$$

and

$$u =$$
$$[-5.336 \ 3.501 \ -7.233 \ 8.233] \begin{pmatrix} \omega_m \\ \omega_d \\ \hat{\tau}_s \\ \hat{w} \end{pmatrix} + 1.835r +$$
$$\rho(e) [0.2428 \ 0.3022 \ 1.247] \begin{pmatrix} \omega_m - r \\ \omega_d - r \\ \hat{\tau}_s - \hat{w} \end{pmatrix}. \tag{38}$$

For comparison, we also design an integration-enhanced CNF controller using the method proposed in [8]:

$$\begin{cases} \dot{x}_i = \omega_d - r, \\ \dot{x}_c = -800 \cdot x_c + 47.06\text{sat } u + [328.4 \ -983.4] \begin{pmatrix} \omega_m \\ \omega_d \end{pmatrix}, \\ \hat{\tau}_s = x_c - [0.2729 \ -1.092] \begin{pmatrix} \omega_m \\ \omega_d \end{pmatrix}, \end{cases} \tag{39}$$

and

$$u =$$
$$[-3.67 \ -4.188 \ 2.336 \ -0.9814] \begin{pmatrix} x_i \\ \omega_m \\ \omega_d \\ \hat{\tau}_s \end{pmatrix} + 1.852r +$$
$$\rho(e) [0.1362 \ 0.4805 \ 0.0669 \ 2.37] \begin{pmatrix} x_i \\ \omega_m - r \\ \omega_d - r \\ \hat{\tau}_s \end{pmatrix}, \tag{40}$$

where the gain function $\rho(e)$ is the same as the one used in the RCNF controller. Moreover, the closed-loop poles are placed at the same locations as of RCNF, with an additional integration pole at $-0.01\omega_n$.

Simulations are conducted to evaluate the performance of the designed controllers. Simulations are first conducted to track two different target speeds, i.e., $r = 10$ rad/s and $r = 30$ rad/s, and the load torque τ_L is set to be 0 initially and then stepped up to 3.5 N·m at the time instant 0.05 s. The simulation results with RCNF are shown in Fig.3 and Fig.4, where the output response is fast and smooth without steady-state error, and the speed ω_d settles down to the target value within 20 ms after the rapid increase of τ_L. Fig.5 and Fig.6 present the simulation results with the integration-enhanced CNF controller, the speed response is also fast and accurate (comparable with that of RCNF) when there is no load torque. However, after the load torque is applied, a noticeable error appears in the speed response and the error cannot be wiped out within a reasonable time. It is possible to redesign this controller for better

rejection of load disturbance. e.g., if we use the integration action $\dot{x}_i = 7.2(\omega_d - r)$ instead and accordingly refresh the feedback gain matrices (going through the design procedure again), we can obtain the simulation results given in Fig.7, with a desirable speed response against the load torque 3.5 N·m, but unfortunately a sustained overshoot appears at the early stage without load torque. Clearly, it is difficult to choose a set of design parameters for the integration-enhanced CNF control to maintain a desirable performance in the presence of various load amplitudes.
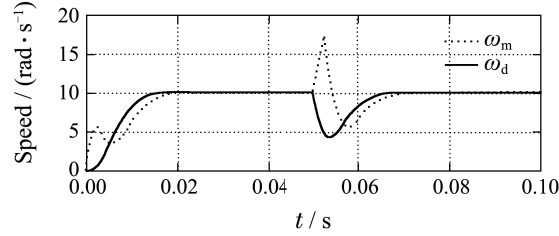
(a) Speed response
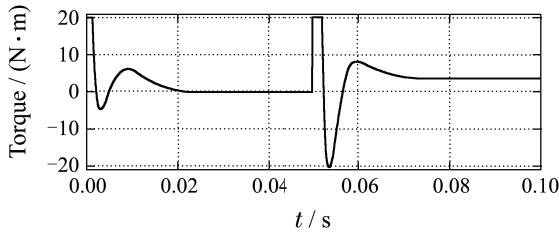
(b) Control signal

Fig. 3 Simulation results with RCNF for target speed
$r = 10$ rad/s
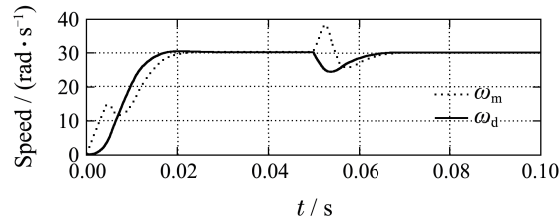
(a) Speed response
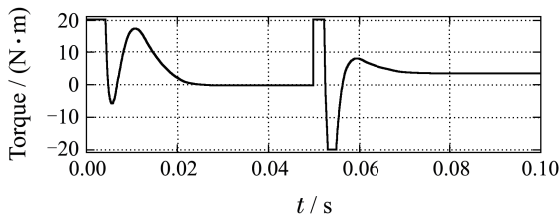
(b) Control signal

Fig. 4 Simulation results with RCNF for target speed
$r = 30$ rad/s

Next, simulation is done for $r = 10$ rad/s with an initial load torque of 3.5 N·m which is removed at the time instant 0.05 s. Again, a fast and accurate tracking performance is obtained by the RCNF controller, as shown in Fig.8. Finally, we study the case when the initial load torque is $\tau_L = 1 + 0.2\sin(20\pi t + \pi/4)$, and an additional 3.5 N·m is superimposed at time instant 0.05 s, and

comparisons are made with a conventional CNF controller (using the same parameters as the RCNF controller, but without the disturbance compensation mechanism, i.e, let $F_w = 0$ and $G_w = 0$) and a linear disturbance-rejection controller (with a dominant damping ratio $\zeta = 0.8$). The results are given in Fig.9. Obviously, the RCNF controller achieves fast and accurate tracking in the face of time-varying disturbance, while the conventional CNF controller leads to a noticeable steady-state error, and the linear controller results in a sluggish closed-loop response.
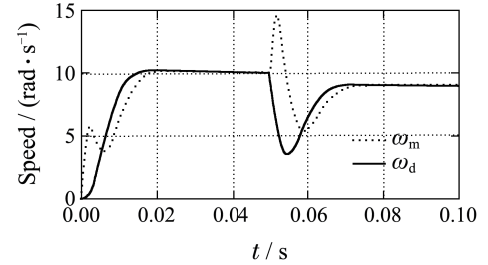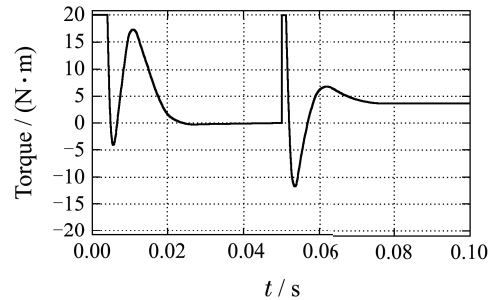

(a) Speed response
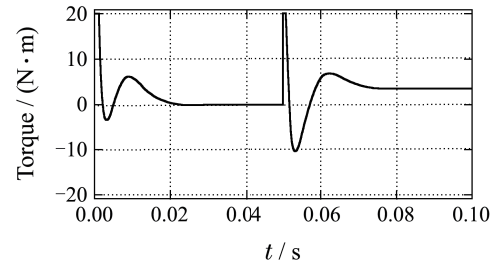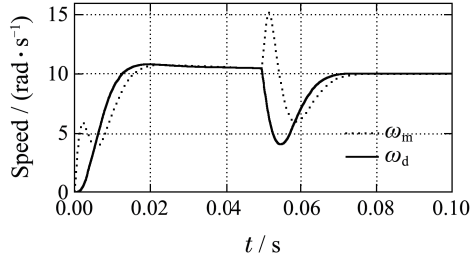

(b) Control signal

Fig. 5 Simulation results with integration-enhanced CNF for
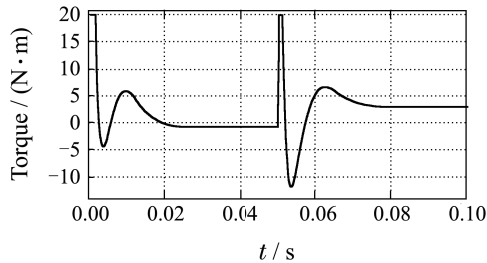target speed $r = 10$ rad/s
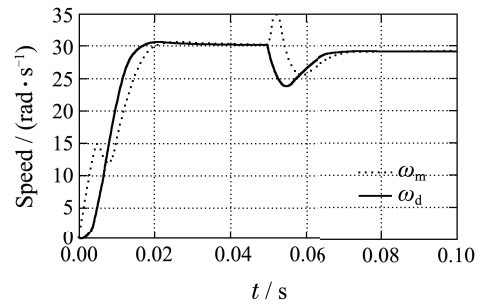
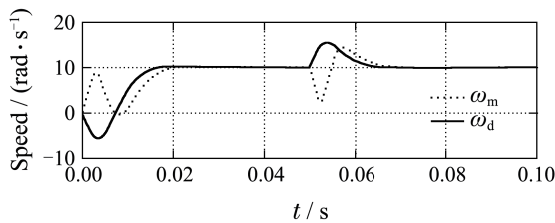(a) Speed response

(b) Control signal

Fig. 6 Simulation results with integration-enhanced CNF for
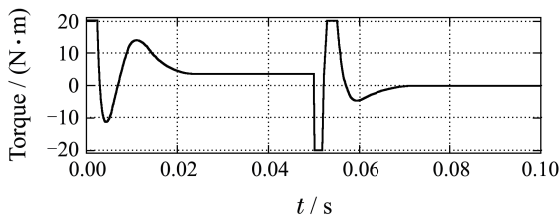target speed $r = 30$ rad/s
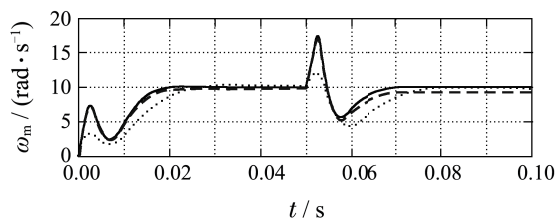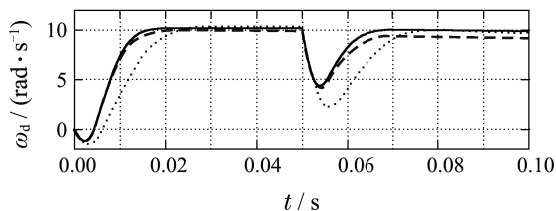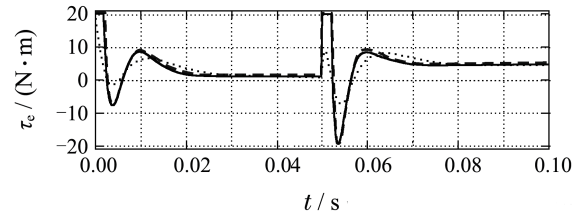
(a) Speed response

(b) Control signal

Fig. 7 Simulation results with integration-enhanced CNF (redesigned) for target speed $r = 10$ rad/s

(a) Speed response

(b) Control signal

Fig. 8 Simulation results with RCNF for target speed $r = 10$ rad/s with initial load torque

(a) Speed response $-\omega_m$

(b) Speed response $-\omega_d$

—— RCNF　　　　--- Conventional CNF
····· Linear control (ξ=0.8)

(c) Control signal $-\tau_e$

Fig. 9 Comparisons among three controllers for target speed $r = 10$ rad/s

5 Conclusion

The design of a disturbance-rejection CNF control method has been presented, which incorporates an extended state observer for both states and disturbance estimation into the CNF control framework. No explicit integration action is needed in the proposed method. This method is able to achieve superior transient and steady-state set-point tracking performance for linear systems with actuator saturation and disturbances. Both matched and unmatched disturbances can be handled elegantly within the unified control framework. Closed-loop stability has been established by strict proof based on Lyapunov theory. This control method was then applied to a two-inertia servo drive system. Simulation results show that the servo system is capable of tracking a wide range of target references fast and accurately, and has a better robustness against the amplitude variations of load disturbance. The control method offers a desirable solution for performance enhancement in industrial servo systems. In this paper, we have been focusing on the set-point tracking problem. To accommodate the case of time-varying references (trajectory tracking), some modifications would be needed. One possible solution is to include a trajectory generator to construct the target state vector (may be varying) for use in the CNF control framework (see e.g., [26]), which can be reserved for a future research.

References:

[1] LU Y S, CHENG C M, CHENG C H. Non-overshooting PI control of variable-speed motor drives with sliding perturbation observers [J]. *Mechatronics*, 2005, 15(9): 1143 – 1158.

[2] OUYANG P R, ZHANG W J, GUPTA M M. An adaptive switching learning control method for trajectory tracking of robot manipulators [J]. *Mechatronics*, 2006, 16(1): 51 – 61.

[3] WANG Y, XIONG Z, DING H. Fast response and robust controller based on continuous eigenvalue configurations and time delay control [J]. *Robotics and Computer-Integrated Manufacturing*, 2007, 23(1): 152 – 157.

[4] SU Y, SWEVERS J. Finite-time tracking control for robot manipulators with actuator saturation [J]. *Robotics and Computer Integrated Manufacturing*, 2014, 30(2): 91 – 98.

[5] CHENG G, HU J. An observer-based mode switching control scheme for improved position regulation in servomotors [J]. *IEEE Transactions on Control Systems Technology*, 2014, 22(5): 1883 – 1891.

[6] LIN Z, PACHTER M, BANDA S. Toward improvement of tracking performance – Nonlinear feedback for linear system [J]. *International Journal of Control*, 1998, 70(1): 1 – 11.

[7] CHEN B M, LEE T H, PENG K, et al. Composite nonlinear feedback control for linear systems with input saturation: theory and an appli-

cation [J]. *IEEE Transactions on Automatic Control*, 2003, 48(3): 427 – 439.

[8] PENG K, CHEN B M, CHENG G, et al. Modeling and compensation of nonlinearities and friction in a micro hard disk drive servo system with nonlinear feedback control [J]. *IEEE Transactions on Control Systems Technology*, 2005, 13(5): 708 – 721.

[9] LAN W, THUM C K, CHEN B M. A hard disk drive servo system design using composite nonlinear feedback control with optimal nonlinear gain tuning methods [J]. *IEEE Transactions on Industrial Electronics*, 2010, 57(5): 1735 – 1745.

[10] CAI G, CHEN B M, PENG K, et al. Comprehensive modeling and control of the yaw channel of a UAV helicopter [J]. *IEEE Transactions on Industrial Electronics*, 2008, 55(9): 3426 – 3434.

[11] PENG K, CAI G, CHEN B M, et al. Design and implementation of an autonomous flight control law for a UAV helicopter [J]. *Automatica*, 2009, 45(10): 2333 – 2338.

[12] CAI G, CHEN B M, DONG X, et al. Design and implementation of a robust and nonlinear flight control system for an unmanned helicopter [J]. *Mechatronics*, 2011, 21(5): 803 – 820.

[13] CHENG G, PENG K. Robust composite nonlinear feedback control with application to a servo positioning system [J]. *IEEE Transactions on Industrial Electronics*, 2007, 54(2): 1132 – 1140.

[14] PARK Y, STEIN J L. Closed-loop state and input observer for systems with unknown inputs [J]. *International Journal of Control*, 1988, 48(3): 1121 – 1136.

[15] SOFFKER D, YU T J, MULLER P C. State estimation of dynamical systems with nonlinearities by using proportional-integral observer [J]. *International Journal of Systems Science*, 1995, 26(9): 1571 – 1582.

[16] FLOQUET T, BARBOT J P. State and unknown input estimation for linear discrete-time systems [J]. *Automatica*, 2006, 42(11): 1883 – 1889.

[17] CHANG J L. Applying discrete-time proportional integral observers for state and disturbance estimations [J]. *IEEE Transactions on Automatic Control*, 2006, 51(5): 814 – 818.

[18] RUBIO J J, MELEMDEZ F, FIGUEROA M. An observer with controller to detect and reject disturbances [J]. *International Journal of Control*, 2014, 87(3): 524 – 536.

[19] ZHENG Q, DONG L, LEE D H, et al. Active disturbance rejection control for MEMS gyroscopes [J]. *IEEE Transactions on Control Systems Technology*, 2009, 17(6): 1432 – 1438.

[20] KIM K, REW K H, KIM S. Disturbance observer for estimating higher order disturbances in time series expansion [J]. *IEEE Transactions on Automatic Control*, 2010, 55(8): 1905 – 1911.

[21] GODBOLE A A, KOLHE J P, TALOLE S E. Performance analysis of generalized extended state observer in tackling sinusoidal disturbances [J]. *IEEE Transactions on Control Systems Technology*, 2013, 21(6): 2212 – 2223.

[22] CHENG G, CHEN B M, PENG K, et al. A MATLAB toolkit for composite nonlinear feedback control-improving transient response in tracking control [J]. *Journal of Control Theory and Applications*, 2010, 8(3): 271 – 279.

[23] SULLIVAN T M O, BINGHAM C M, SCHOFIELD N. Enhanced servo-control performance of dual-mass systems [J]. *IEEE Transactions on Industrial Electronics*, 2007, 54(3): 1387 – 1399.

[24] ERENTURK K. Nonlinear two-mass system control with sliding-mode and optimised proportional-integral derivative controller combined with a grey estimator [J]. *IET Control Theory and Application*, 2008, 2(7): 635 – 642.

[25] ERENTURK K. Fractional-Order PID and active disturbance rejection control of nonlinear two-mass drive system [J]. *IEEE Transactions on Industrial Electronics*, 2013, 60(9): 3806 – 3813.

[26] CHENG G, PENG K, CHEN B M, et al. Improving transient performance in tracking general references using composite nonlinear feedback control and its application to high-speed XY–table positioning mechanism [J]. *IEEE Transactions on Industrial Electronics*, 2007, 54(2): 1039 – 1051.

作者简介:

　　程国扬　(1970–), 男, 博士, 教授, 研究方向为先进控制技术及其在机电系统中的应用, E-mail: cheng@fzu.edu.cn;

　　黄宴委　(1976–), 男, 博士, 副教授, 研究方向为机器视觉、智能控制、电力系统自动化, E-mail: sjtu‿huanghao@fzu.edu.cn.